

A filter free dual transmission grating spectrometer for the extreme-ultraviolet

Seth R. Wieman^{*a}, Leonid V. Didkovsky^a, Darrell L. Judge^a, Andrew R. Jones^b, Matthew Harmon^b

^a Univ. of Southern Calif.; Space Sciences Center; SHS-274; UPC; Los Angeles, CA 90089;

^b University of Colorado, Boulder; LASP; 1234 Innovation Dr.; Boulder, CO 80303

ABSTRACT

We report the design and laboratory testing of a prototype dual-grating filter-free extreme ultraviolet (EUV) spectrometer that has potential as a highly stable instrument for measuring absolute solar irradiance in the X-ray through far ultraviolet spectral range. The instrument is based on the same freestanding transmission gratings and silicon photodiodes used on the successful Solar EUV Monitor (SEM) aboard SOHO and the EUV Spectrophotometer (ESP) part of the EVE instrument suite to be flown on SDO. Its two gratings, placed in series, along with a simple baffle structure provide excellent out of band “white” light rejection. Because the instrument does not use any thin film filters or reflective optics it is not susceptible to the degradation and instability associated with such optical elements. We present photometric efficiency data from laboratory tests with a Helium and Hydrogen discharge light source and measurements of “white” light rejection taken using the Mt Wilson Observatory 60’ solar telescope.

Keywords: EUV, transmission grating, spectrophotometer, spectrograph, photometer

1. INTRODUCTION

Long-term stable measurements of solar flux in the highly variable X-ray, extreme ultraviolet (EUV) and far ultraviolet (FUV) spectral regions are key to understanding the science and photochemistry underlying many solar system phenomena and require instrumentation that is not susceptible to degradation and time-dependent change¹. However, to monitor solar EUV against a background of far more intense visible light, EUV spectrometers conventionally rely on thin metal film filters, which suffer from long-term stability problems. Specifically, transmission characteristics of thin film filters may change over time^{2,3} due to an interaction with chemical elements, e.g., carbon and may develop pinholes due to the impact of ambient particles. Some additional problems with thin film filters are that they typically have multiple bandpasses for a given film and do not allow precise selection of the desired wavelength band of interest.

We report the design and testing of a prototype EUV spectrometer that does not use thin film filters but instead suppresses background visible light through the use of two freestanding transmission gratings in series (i.e., the incoming EUV radiation is diffracted twice before reaching the detector). This instrument is an enhanced version of our CELIAS Solar EUV Monitor (SEM) instrument aboard SOHO, which uses a single transmission grating and two thin film filters in series to eliminate pinhole overlap and thereby eliminate visible light detection. Having provided EUV irradiance measurements for over 11 years now, SEM has proven to be a highly stable, robust spectrometer, but has, nevertheless, suffered minor degradation related mainly to carbon deposition on its Al filter.

Freestanding gratings of the type used in our spectrometer are the subject of considerable previous research⁴⁻⁹. They have been used successfully on space flight missions including SOHO^{6,7} and multiple sounding rocket flights⁸, and their diffracting^{5,9}, polarizing¹⁰⁻¹² and wave-guide^{5,13} properties have been investigated. The gratings consist of a set of parallel gold bars, separated by gaps, and supported by larger scale nickel mesh as shown in Figure 1. Gratings with 400 nm and 600 nm periods are used in the prototype reported here. The grating with the 400 nm period has a bar to gap width ratio of 0.8 and thickness of 470 nm. The bar to gap width ratio for the 600 nm period grating is 1.0 and its thickness is 490 nm. These gratings were selected from a limited number that were available to us at the time of these tests, and were not formally optimized based on line density, bar to gap ratio, and thickness, all of which effect transmission. The DGS signal to noise and signal to background ratios reported below could be improved by such an optimization. The gratings

* wieman@usc.edu; phone 1 213 740 5751; fax 1 213 740 6342;

were fabricated at Massachusetts Institute of Technology using a holographic lithography technique described in detail in Schattenburg et al¹⁴.

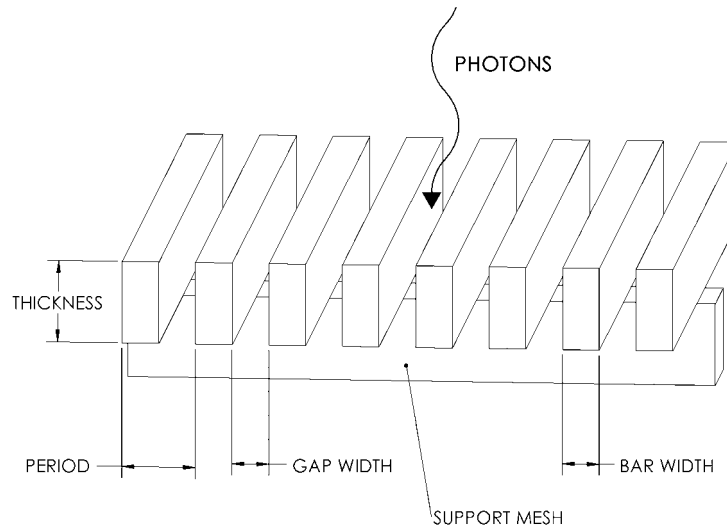


Fig. 1. Schematic view of a freestanding transmission grating

Here we assess how effectively the dual-grating spectrometer (DGS) isolates resonance lines of helium at 58.4 nm and hydrogen at 121.6 nm (Lyman- α) from the rest of the solar spectrum based on two sets of measurements. First, the DGS transmission at these EUV wavelengths is measured using a gas glow discharge lamp and vacuum monochromator as a light source. Second, the degree to which solar “white” light (as stray light within the optics cavity or as scatter directly off of the gratings) reaches the DGS detector is determined with a similar set of measurements made using the 60’ solar telescope at Mt Wilson Observatory - a light source that is comparable in spectral content to the light that it would be necessary to reject in space-based solar measurements. The DGS instrument used in these tests is described in section 2. The procedure for the transmission measurements is described in Section 3. In section 4, the results of these measurements are presented along with a discussion of what they suggest about the instruments’ performance in space-based solar measurements. Concluding remarks are in the summary.

2. INSTRUMENT DESCRIPTION

The laboratory dual grating spectrometer (DGS) prototype (Figure 2) consists of a hermetically sealed optics cavity with 2 transmission gratings (labeled G1 and G2, respectively, in Figure 2) and an uncoated EUV sensitive silicon photodiode detector (the “primary” detector, labeled D1). Initial dispersion of incoming radiation is achieved with grating G1, positioned immediately behind a 1 mm Δ 10 mm entrance slit. The EUV spectral radiation is then diffracted a second time through Grating G2, centered on the first diffracted order from G1, before reaching detector D1. The primary detector and its aperture (the spectrometer exit slit) are mounted on a linear translation stage that allows them to be scanned (along the x-axis) through the diffraction pattern produced by G2. Selectable and removable light baffles consisting of blackened plates with knife-edged apertures along the series of +1, +1[†] and +1, 0 order beam paths between G2 and D1 and along the +1 order beam path between G1 and G2 (see Figure 2) help control scattered light in the DGS cavity. The baffles are placed such that when the detector is centered on the +1, +1 order from G2, it does not have a direct line of sight to G1; the baffles thus shield the detector from visible light scattered directly from G1. The DGS is configured for different EUV bandpasses by repositioning the gratings, baffle structure, and the detector.

[†] In this report we designate spectral orders in the diffraction pattern produced by grating G2 using 2 numbers. For example, the +1,0 order would indicate the 0 spectral order that is produced when the +1 order from grating G1 is diffracted by grating G2 (see Figure 2).

A second “reference” photodiode detector (an International Radiation Detectors AXUV photodiode of the same model and manufacturing lot as the primary detector) is positioned in front of and slightly beneath the DGS entrance such that the light source illuminates both the DGS entrance and the reference detector simultaneously. The reference photodiode is used as a monitor for changes in source intensity. If the source intensity should drift while the primary detector is being scanned, for example, the reference diode photocurrent (measured concurrently throughout the scan) can be used to measure changes in the primary diode signal due to a source intensity drift, and thus remove such changes from the true wavelength dependent diode signal level.

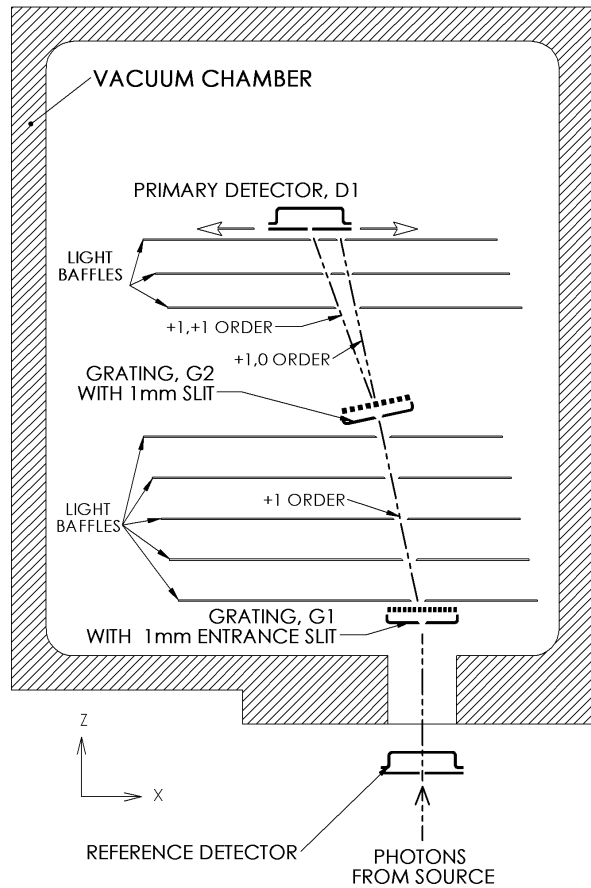


Fig. 2. Schematic of spectrometer optics – The DGS uses 2 transmission gratings, 2 detectors (a “primary” detector to monitor transmission through the gratings and a “reference” detector, which intercepts a portion of the incident beam, to monitor changes in light source intensity) and a series of removable light baffles. The scaled 58.4 nm configuration is shown here; when configured for 121.6 nm the light baffles between G2 and the primary detector have apertures for the +1, +1 order only.

The reference detector and the ability to translate the primary detector are features that were incorporated into the prototype to assist in the laboratory tests of the instrument and would not likely be included in a space flight version of the spectrometer. In a flight version, the primary detector would be in a fixed position centered on the +1, +1 order from grating G2. For simultaneously measuring multiple wavelength bands of interest, additional detectors, exit slits and baffle apertures would be used (depending on the range of diffraction angles from G1, additional secondary gratings may be required as well). The absolute sensitivity of the instrument would be determined using a stable, calibrated EUV source such as a synchrotron. Without the laboratory features, the mass of a space-based version of the spectrometer could be kept below 1000 g.

Two different DGS spectral window configurations were tested. In the first configuration, the gratings and baffles were positioned to transmit 58.4nm radiation in the +1, +1 order with a 400 nm period grating in the G1 position and a 600 nm period grating in the G2 position. In the second configuration, the same gratings were used, but were positioned to transmit 121.6 nm radiation. The instrumental line profiles (Figure 3) with the detector centered on the +1, +1 order were modeled for these two configurations by a simple ray trace based on the known general diffraction grating formula: $m\lambda = p[\sin(\theta_i) + \sin(\theta_d)]$ where p is the grating period, m is diffraction order, λ is wavelength, and θ_i and θ_d are the angle of incidence and the angle of diffraction, respectively. Based on these profiles, the spectrometer resolution (bandpass FWHM) is approximately 3 nm for both configurations.

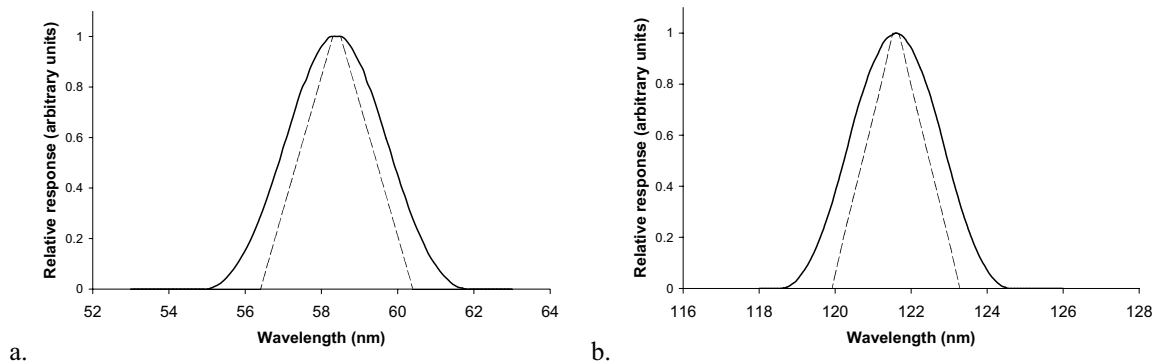


Fig. 3. Instrumental line profiles (thick line) and slit functions (dashed line) for the modeled DGS configured for monitoring a. 58.4 nm and b. 121.6 nm EUV

3. TRANSMISSION MEASUREMENTS

3.1 EUV Transmission

The DGS transmission for 58.4 nm and 121.6 nm EUV was measured in the laboratory using a 0.5m Seya-Namioka type vacuum monochromator with a helium/hydrogen DC glow-discharge light source (shown in Figure 4). The monochromator uses a concave reflection grating with 1200 lines/mm blazed at 70 nm.

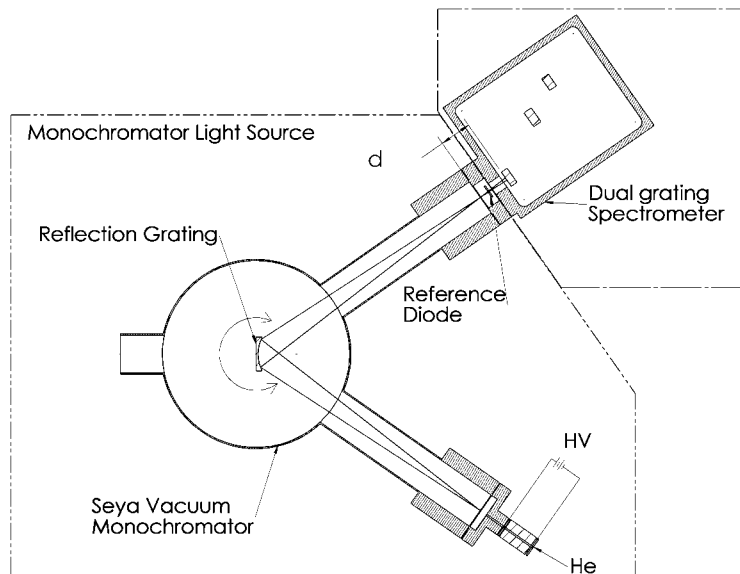


Fig. 4. Laboratory setup for testing the Dual Grating Spectrometer EUV transmission

The distance d in Figure 4, from the monochromator exit slit (focal plane) to the DGS entrance slit, was set such that the beam entering the DGS has a divergence of approximately 0.5° ($.25^\circ$ each side of center).

Transmission, T , for the two gratings in series is defined as I_1/I_0 , where I_0 is the EUV intensity at the spectrometer entrance slit, and I_1 is the intensity of EUV reaching the detector backplane behind G2. Because the same detector is used to measure intensity at both locations (the primary detector, which measures I_1 at position D1, is relocated to the G1 position to measure I_0), the photon detection efficiency of the detector can be eliminated from the calculation of I_1/I_0 . Since the two measurements cannot be obtained simultaneously, they are normalized based on their respective concurrent reference diode signal to account for any changes in beam intensity. Thus, transmission at a given detector scan position in the diffraction pattern from G2 is given by:

$$T_X = \left| \frac{I_1}{I_0} \right| = \frac{i_{p1}/i_{r1}}{i_{p0}/i_{r0}} \quad (1)$$

where: i_{p1} is the primary diode photocurrent while at a given scan position behind G2, i_{r1} is the reference diode photocurrent measured simultaneously with i_{p1} , i_{p0} is the primary diode photocurrent while positioned immediately behind the entrance slit and i_{r0} is the reference diode photocurrent measured simultaneously with i_{p0} . Detector dark currents are subtracted from photocurrent measurements.

The use of the reference detector as a means of preventing changes in source intensity from influencing final transmission values requires that for a given primary diode position, the photocurrent ratio i_p/i_r be a fixed value (the primary and reference detectors must respond linearly to changes of source intensity). Therefore, for critical primary diode positions (in particular, the central position directly behind the entrance slit and the position centered on the 1st order from G2) this ratio was established through several hundred measurements for which the source intensity was deliberately varied over approximately 1 order of magnitude by adjusting the source input power and helium/hydrogen flow rate. The mean value was used in the transmission calculations, and standard deviation from the mean for all measurements at a given primary diode location were typically less than 3% of the mean value.

3.2 Solar “white” light transmission

Measurements of DGS solar “white” light transmission (suppression) were made at the 60’ solar telescope at Mt. Wilson Observatory. The telescope projected a collimated solar image on the DGS entrance slit. The DGS reference diode aperture and spectrometer entrance slit occupied an area approximately 12mm Δ 1mm at the center of the 36 mm solar image. Apart from the change in light source, the white light measurements were made using exactly the same spectrometer configuration (grating and baffle positions) and detector scan range that were used in the 58.4 nm measurements. Additional scans were performed with a polarizing filter placed immediately in front of the DGS entrance to measure the effect of polarization angle on transmission. Vertical (parallel to grating bars), horizontal and several intermediate polarization angles at 15° increments were measured.

As of the time of this report, solar white light transmission at Mt. Wilson had not yet been made with the DGS in its 121.6 nm configuration. In lieu of these measurements visible light transmission measurements were made using an intense tungsten halogen lamp (sun gun) in the laboratory. The tungsten halogen lamp has poorer collimation and beam uniformity than the solar source, so its transmission is not likely to be equivalent. It does, however, illustrate the general shape of the transmission profile across the detector scan plane.

4. RESULTS AND DISCUSSION

Figure 5 shows the EUV and solar “white” light transmission profiles (e.g. transmission vs. detector scan position) for the 58.4 nm configuration. The scan position values on the horizontal axis have an arbitrary origin and increase as the detector moves in the direction of the entrance slit (e.g., towards grating G1 zero order). Peaks for +1, +1 and +1, 0 orders can be seen in the 58.4 nm profile (thick black line). The transmission profile for solar white light measured at Mt. Wilson over the same scan range is plotted on the same horizontal axis, but with a different vertical scale for direct illumination with no polarizing filter (thick gray line) as well as for illumination with light polarized in the vertical and

45° (thin dashed and thin dotted lines respectively) directions. The profiles for the polarized and non-polarized beams are virtually indiscernible, suggesting that polarization has very little effect on transmission for this spectral region. The edges of the baffle structure +1, +1 order and +1, 0 order windows projected onto the detector plane are shown for reference. The Scan position labeled A, at the center of the +1, +1 order peak, is the location at which the transmission of 58.4 nm EUV is the greatest relative to that of white light. This location is where the detector would be fixed for solar observations at 58.4 nm.

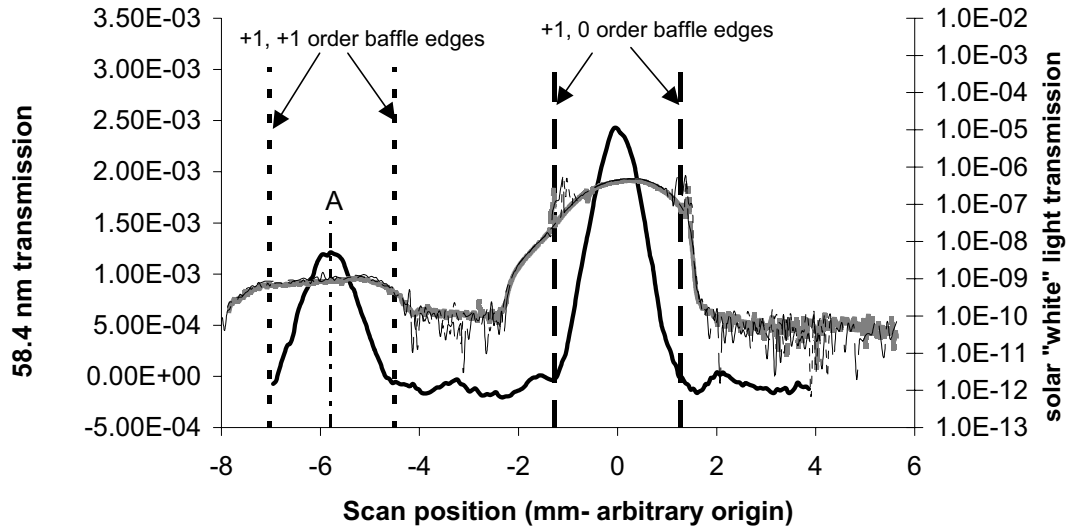


Fig. 5. DGS Transmission profiles for solar white light (thick gray line) and 58.4 nm EUV (thick black line). The thin dashed line and thin dotted line indicate transmission for light polarized in the vertical and 45° directions respectively. Scan position labeled A is the position at which the ratio of transmission for 58.4 nm relative to solar white light is greatest.

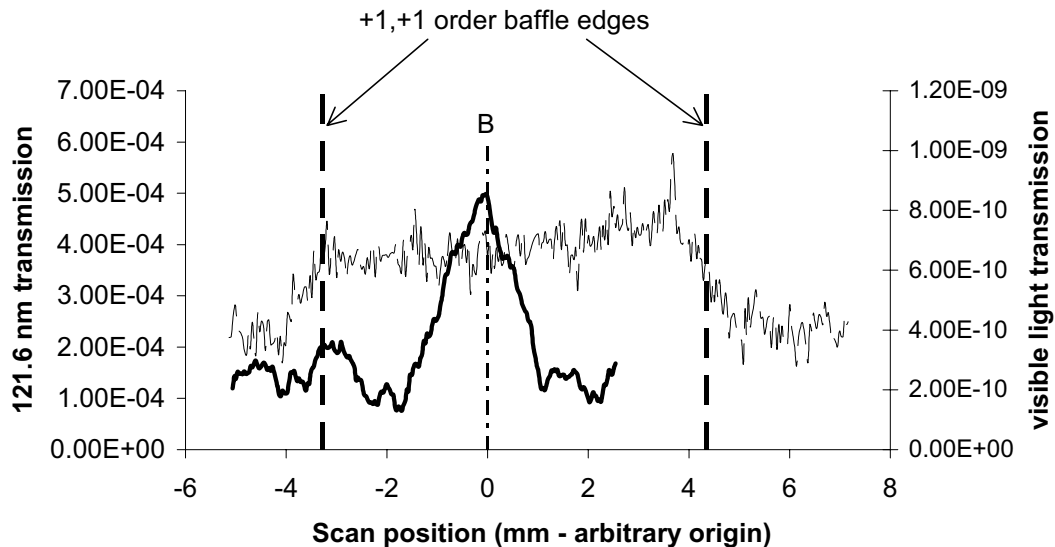


Fig. 6. DGS Transmission profiles for solar white light (thin line) and 121.6 nm EUV (thick line). The scan position labeled B is the position at which the ratio of transmission for 121.6 nm EUV relative to solar white light is greatest

Transmission profiles for the Lyman- ζ 121.6 nm DGS configuration are shown in Figure 6. Because of the larger dispersion angles for Lyman- ζ , the detector translation stage has insufficient travel to cover both the +1, +1 and the +1, 0 orders in a single scan, so only the +1, +1 order is shown in the 121.6 nm transmission profile (thick line). The visible light transmission profile was measured using a tungsten halogen lamp as described above. The Scan position labeled B, at the center of the +1, +1 order peak is the location at which the transmission of the 121.6 nm FUV is the greatest relative to that of white light. This location is where the detector would be fixed for solar observations at 121.6 nm.

The above measurements, along with the solar intensity in the EUV band of interest relative to that of the full solar spectrum (within the range of sensitivity of the detector), indicate the signal to background ratio that the DGS could achieve in space-based measurements. This “signal to background ratio” (SBR) indicates how effectively the spectrometer isolates the particular spectral band of interest, but is different from a signal to **noise** ratio, in the sense that it is a measure of the strength of the desired signal relative to a background signal which is proportional to the “solar constant” and therefore quite stable. The detected DGS signal related to a given solar spectral band is proportional to the integral of DGS transmission, T_{DGS} , detector efficiency, ξ_{det} , and solar spectrum intensity, I_{solar} (all are wavelength dependent) over the specified spectral window. Therefore, the SBR, for a specified EUV spectral band, ζ_1 to ζ_2 measured against the broader solar spectrum ranging from ζ_3 to ζ_4 is given by:

$$SBR = \frac{\int_{\zeta_1}^{\zeta_2} \xi_{det} T_{DGS} I_{solar} d\zeta}{\int_{\zeta_3}^{\zeta_4} \xi_{det} T_{DGS} I_{solar} d\zeta} \quad (2)$$

The DGS EUV and white light transmission values measured with the detector centered on the +1, +1 order provide bulk constants, T_{EUV} and T_{white} which represent T_{DGS} integrated over the respective EUV and white light bands of interest. Equation (2) can be expressed in terms of T_{EUV} and T_{white} as:

$$SBR = \frac{T_{EUV} \int_{\zeta_1}^{\zeta_2} \xi_{det} I_{solar} d\zeta}{T_{white} \int_{\zeta_3}^{\zeta_4} \xi_{det} I_{solar} d\zeta} \quad (3)$$

SBR values for the 58.4 nm and 121.6 nm configurations are presented in Table 1. The integrals of detector efficiency and spectral intensity over wavelength are computed based on detector efficiency data from the manufacturer, Korde¹⁶ and from Krumrey¹⁷ et al. and on solar spectrum data (for worst case solar minimum) from Tobiska¹⁸ et al. Uncertainty in transmission values is related primarily to the I_1 measurements for which the photocurrents were typically quite low (sometimes only a few times greater than the detector noise level).

The expected signal to **noise** ratio (EUV signal to total noise) during space based solar observations is also shown in Table 1. The EUV signal level is equal to the numerator from (3) multiplied by the area of the DGS entrance slit (10 mm²). The noise level is dependent on the electronics and diode stability and can be reduced to less than 50% of the EUV signal even for the less intense 58.4 nm line at solar minimum.

Table 1. Summary of measured transmission values at the +1, +1 order and expected signal to background and signal to noise ratios for 58.4 nm and 121.6 nm DGS configurations for space based solar observations (calculated for solar minimum)

DGS Configuration	EUV bandpass (nm-FWHM)	EUV Transmission, T_{EUV}	White light Transmission, T_{white}	Expected SBR	Expected SNR
58.4 nm	57-60	8.8e-4 +/- 5e-6	9e-10 +/- 1e-10	.04	2
121.6 nm	120-123	3.3e-4 +/- 5e-6	9e-10 +/- 1e-10	1.2	70

Although a value of T_{white} for the 121.6 nm configuration was not measured using the solar telescope at Mt. Wilson Observatory a reasonable estimate of this constant can be made based on its value for the 58.4 nm configuration. The DGS has the same gratings and the same general baffle structure when configured for 121.6 nm that it has when configured for 58.4 nm; these components are merely shifted to allow for the larger diffraction angles associated with the longer wavelength. Furthermore, measurements of white light transmission for a well-collimated normal incident beam through a single grating (Figure 7) show that transmission decreases rapidly as the transmission angle (e.g. the angle that the path from grating to detector forms with the grating normal) increases. Because the detector and grating G2 lie at angles farther from the grating G1 normal for the 121.6 nm configuration, it is reasonable to assume that the white light transmission through this configuration will be even lower than through the 58.4 nm configuration. To be conservative, however, a 121.6 nm T_{white} value equal to that for 58.4 nm was used to calculate the SBR value reported in Table 1.

One cannot conclude from these measurements what portion of the residual solar white light signal is from stray light within the optical cavity that eventually reaches the detector after multiple reflections and what portion is due to light scattering off of the gratings directly to the detector through the baffle apertures. If a significant portion of the residual white light signal is due to stray light, it is likely that improving the baffle structure could further reduce white light transmission. However, if the remaining signal is due primarily to direct scatter off of the gratings (e.g. a characteristic of the gratings which could not be easily changed) it is not likely that white light rejection can be significantly improved. We intend to further investigate which of these mechanisms has a greater effect. Our planned approach for this investigation is to install a set of light traps at the 0 and +1, 0 orders to limit the amount of indirect stray light reaching the detector.

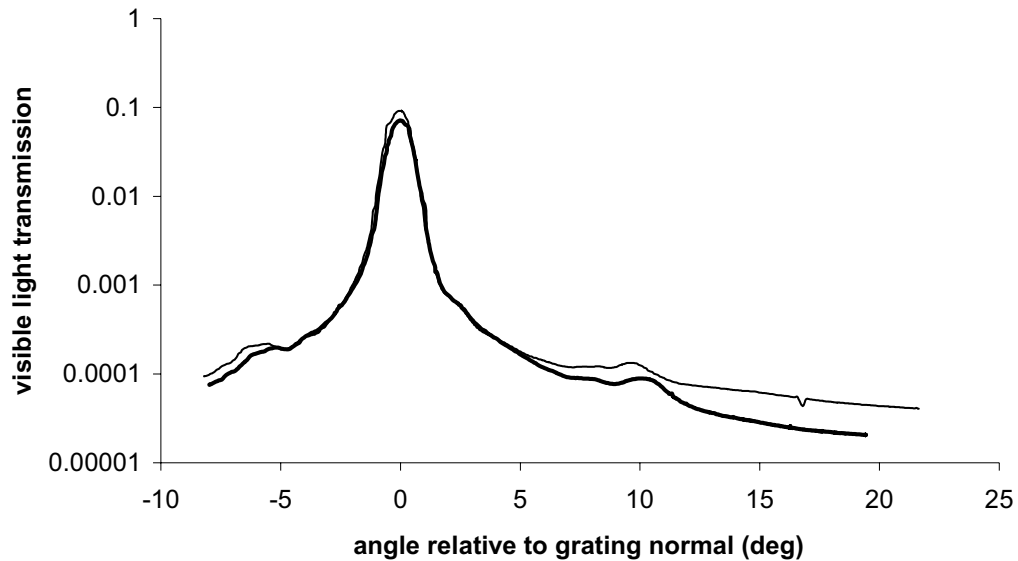


Fig. 7. Visible light transmission through a 400nm period grating (thick line) and a 600 nm grating (thin line) versus transmission angle measured relative to grating normal

5. SUMMARY

We have presented the design and testing of an EUV spectrometer based on two highly stable freestanding transmission gratings placed in series, and silicon photodiodes that achieves excellent white light rejection ($>10^9$) without the use of degradable thin film filters. As a measure of how effectively the spectrometer can isolate EUV lines from the much

brighter visible white light portion of the solar spectrum, we have measured the signal to background ratio that the instrument is expected to achieve for solar measurements of the He 58.4 nm resonance line and estimated it for the hydrogen Lyman- line. Based on our measurements and estimates it appears that the dual transmission grating spectrometer offers a very appealing alternative to filter based EUV spectrometers.

ACKNOWLEDGEMENTS

This work has been supported in part by NASA Grant NAG5-11807. We would like to thank Ed Rhodes, Perry Rose and Andy Grubb for their time, expertise and assistance with the measurements at Mt. Wilson Observatory.

REFERENCES

1. M. D. Daybell, M. A. Gruntman, D. L. Judge, J. A. R. Samson, "Rare-gas optics-free stable extreme-ultraviolet photon spectrometer for solar system studies," *Optical Engineering*, 33(2), 445-450 (1994)
2. J. V. Vallerga, P. W. Vedder, O. H. W. Siegmund, "Experiences with thin-film filter development for the extreme ultraviolet explorer," *SPIE Proceedings*, 1742(1), 392-402 (2004)
3. F. R. Powell, J. F. Lindblom, S. F. Powell, P. W. Vedder, "Thin film filter performance for extreme ultraviolet and x-ray applications," *Optical Engineering* 29(6), 614-624 (1990)
4. M. L. Schattenburg, "From nanometers to gigaparsecs: The role of nanostructures in unraveling the mysteries of the cosmos," *Journal of Vacuum Science & Technology B: Microelectronics and Nanometer Structures* 19(6), 2319-2328 (2001)
5. D. R. McMullin, D. L. Judge, C. Tarrío, R. E. Vest, F. Hanser, "Extreme-Ultraviolet Efficiency Measurements of Freestanding Transmission Gratings," *Applied Optics*, 43(19), 3797-3801 (2004)
6. H. S. Ogawa, D. R. McMullin, D. L. Judge, R. S. Korde, "Normal incidence spectrophotometer with high-density transmission grating technology and high-efficiency silicon photodiodes for absolute solar extreme-ultraviolet irradiance measurements," *Optical Engineering*, 32(12), 3121-3125 (1993)
7. D. L. Judge, D. R. McMullin, H. S. Ogawa, D. Hovestadt, B. Klecker, M. Hilchenbach, E. Möbius, L. R. Canfield, R. E. Vest, R. Watts, C. Tarrío, M. Kühne and P. Wurz, "First Solar EUV Irradiances Obtained from SOHO by the Cielas/Sem," *Solar Physics*, 177(1), 161-173 (1998)
8. D. L. Judge, D. R. McMullin, H. S. Ogawa, "Absolute solar 30.4 nm flux from sounding rocket observations during the solar cycle 23 minimum," *Journal of Geophysical Research*, 104(A12), 28321-28324 (1999)
9. H. Lochbihler, P. Predehl, "Characterization of x-ray transmission gratings," *Applied Optics*, 31(7), 964-971 (1992)
10. M. Gruntman, "Extreme-ultraviolet radiation filtering by freestanding transmission gratings," *Applied Optics* 34(25), 5732-5737 (1995)
11. E. E. Scime, D. J. McComas, E. H. Anderson, M. L. Schattenburg, "Extreme-ultraviolet polarization and filtering with gold transmission gratings," *Applied Optics*, 34(4), 648-654 (1995)
12. M. M. Balkey, E. E. Scime, M. L. Schattenburg, and J. van Beek, "Effects of Gap Width on Vacuum-Ultraviolet Transmission Through Submicrometer-Period, FreeStanding Transmission Gratings," *Appl. Opt.* 37, 5087-5092 (1998)
13. N. M. Ceglio, A. M. Hawryluk, D. G. Stearns, M. Kuhne, P. Muller, "Demonstration of guided-wave phenomena at extreme-ultraviolet and soft-x-ray wavelengths," *Optics Letters*, 13(4), 267-269 (1988)
14. M. L. Schattenburg, E. H. Anderson, H. I., "X-ray/VUV transmission gratings for astrophysical and laboratory applications," *Phys Scripta* 41, 13-20 (1990)
15. R. Korde, www.ird-inc.com
16. M. Krumrey, C. Herrmann, P. Müller, and G. Ulm, "Synchrotron-radiation-based cryogenic radiometry in the x-ray range," *Metrologia* 37, 361-364 (2000).
17. K. Tobiska, www.spacewx.com